

1 **Ground Motion Prediction Equations for Application to the 2015 Canadian National Seismic**  
2 **Hazard Maps**

3

4 **Can. J. Civ. Eng. Revised April 2013**

5 Gail M. Atkinson<sup>1</sup> and John Adams<sup>2</sup>

6 (1. Western University, London, [gmatkinson@aol.com](mailto:gmatkinson@aol.com);

7 2. Geological Survey of Canada, [jadams@nrcan.gc.ca](mailto:jadams@nrcan.gc.ca) )

8

9 **Abstract**

10

11 Ground-motion prediction equations (GMPEs) and their epistemic uncertainty are a key input to seismic  
12 hazard assessments, because the GMPEs specify the expected ground-shaking amplitudes as a function  
13 of magnitude and distance. We describe a simple and efficient approach to the definition of GMPEs and  
14 their epistemic uncertainty for use in seismic hazard mapping in Canada. The approach defines a lower,  
15 central, and upper GMPE for each type of event (eastern crustal, western crustal, interface, in-slab,  
16 offshore) that contributes to the hazard, by considering alternative published GMPEs and data that may  
17 be used to constrain these model choices. The proposed model is being applied in trial seismic hazard  
18 maps for Canada, for consideration in the 2015 edition of the National Building Code of Canada  
19 (NBCC2015).

20

21 **Introduction**

22

23 This paper summarizes a model for specifying ground-motion prediction equations (GMPEs) and their  
24 epistemic uncertainty, as proposed for use in new national seismic hazard maps of Canada currently  
25 under development by the Geological Survey of Canada (Adams, 2011). The GMPEs, giving median  
26 ground motion amplitudes as a function of magnitude and distance, are a key component of the seismic  
27 hazard maps in terms of their impact on results. Thus the choice of the GMPEs for input to the seismic  
28 hazard mapping program is very important. Equally important is the range of alternative models used to  
29 capture epistemic uncertainty in the median predicted ground motions for a given magnitude and  
30 distance, expressing a subjective evaluation of the limitations of our current knowledge. This range has  
31 important implications for the calculated ground-motion values which are intended for use in

32 NBCC2015. The method used here may be generally applicable for national seismic hazard maps  
33 (where a large number of possible GMPEs need to be represented by a few alternatives to reduce  
34 computational time) or for site-specific-seismic hazard analyses where simple weighted combinations of  
35 available GMPEs are judged to be inadequate to capture the epistemic uncertainty.

36

37 The recommendations contained herein were prepared for use in new national seismic hazard maps,  
38 being developed at the Geological Survey of Canada, based on ongoing discussions within the seismic  
39 hazard working group of the Canadian Standing Committee on Earthquake Design (members of this  
40 development group are listed in the Acknowledgements). Further documentation, including many  
41 exploratory plots and additional details, can be found in Atkinson (2012).

42

43 This study was motivated by the need to update the GMPEs used in the last national seismic hazard  
44 maps (see Adams and Halchuk, 2003; these GMPEs included Boore et al., 1997, Youngs et al., 1997 and  
45 Atkinson and Boore, 1995) to reflect the last 15 years of developments in the ground-motion field.  
46 During this time period, the databases on which GMPEs are based have grown many-fold, and thus the  
47 changes in knowledge have been significant.

48

49 We overview the GMPEs proposed for use in eastern Canada (crustal events), for crustal earthquakes in  
50 western Canada, for earthquakes offshore of western Canada, and for the two types of subduction zone  
51 earthquakes in southwestern British Columbia (B.C.) , those within the subducted slab (inslab) and those  
52 great earthquakes on the plate interface. The median GMPEs and alternatives to them are discussed  
53 separately from the issue of the appropriate ‘sigma’ (standard deviation about the median), which  
54 follows the discussion of the median equations. It is noted that the proposed model will be  
55 implemented for trial hazard map calculations, and the sensitivity of those calculations to alternative  
56 approaches to modeling GMPEs and their epistemic uncertainty will also be investigated; those  
57 investigations will be reported in a separate study.

58

59 As a prelude to the principles below, we note that epistemic uncertainty in median GMPEs has often  
60 been modeled by the use of alternative equations (typically those derived by various authors), with  
61 model weights being used to represent the relative confidence in each alternative. However, this is not  
62 necessarily the best way to model epistemic uncertainty in GMPEs (see Bommer and Scherbaum, 2008;

63 Atkinson, 2011). To the extent feasible, we prefer to use the alternative GMPEs and applicable data to  
64 guide the choice of a representative or “central” GMPE, and to define representative (upper and lower)  
65 GMPEs that express uncertainty about the central GMPE. We believe this approach offers more  
66 flexibility in expressing uncertainty in knowledge of the correct median GMPE than any weighted  
67 combination of the available GMPEs. We note that a similar approach was used for eastern ground  
68 motions in NBCC2005 and 2010 (Atkinson, 1995) while a simplified approach following the same  
69 general philosophy was used for the western crustal ground motions (see Adams and Halchuk, 2003).

70  
71 The use of representative GMPEs rather than a weighted combination of alternative GMPEs is  
72 undoubtedly the most controversial aspect of the GMPE models we propose herein. This has been a  
73 hotly-debated topic at recent workshops and conferences (e.g. 2012 U.S. Geological Survey workshops  
74 on the 2014 hazard maps in the U.S., and 2012 workshops on specific industry projects), and there is no  
75 clear consensus. Different approaches have different advantages and disadvantages. Proponents of the  
76 alternative GMPE approach argue that use of multiple models with alternative functional forms is  
77 required in order to properly capture uncertainties in form as well as amplitudes, whereas the use of the  
78 representative GMPE approach involves arbitrary judgments concerning the best central model and its  
79 uncertainty. On the other hand, the representative equation approach employed here allows explicit  
80 judgments to be exercised regarding magnitude and distance scaling and the extent to which the selected  
81 models will satisfy data constraints that are important to the project; moreover, it allows control over  
82 how both the median GMPEs and their uncertainty will behave across regions and event types. Thus we  
83 can ensure that the epistemic uncertainty is larger in regions with poorer data, for example, regardless of  
84 whether alternative published GMPEs coincidentally happen to be similar. Furthermore, the  
85 representative GMPE approach has flexibility to accommodate important points that cannot be properly  
86 handled with the weighted-alternative GMPE approach. For example, many GMPEs are appropriate for  
87 some but not all of the magnitude-distance ranges needed, and are therefore not reasonable for general  
88 application (e.g. only two of four recent crustal GMPEs from the PEER-NGA suite are suitable for  
89 small-to-moderate magnitudes, and at regional distances needed for hazard calculations in western  
90 Canada). Finally, the representative equation approach has significant practical utility, enabling a  
91 complex problem to be represented by a minimum number of branches for hazard calculations, which is  
92 efficient and transparent. Admittedly, there is a large degree of judgment exercised regarding the  
93 selection of the central model and its upper and lower branches, and this exerts significant influence on

94 the hazard results. However, such subjective judgments are equally important when using the  
95 alternative-GMPE approach, as the selection and weighting of alternative models is also a process based  
96 on subjective judgment. Ultimately, it is important to document the rationale for the approach taken,  
97 which is provided herein. Furthermore, we note we have performed numerous sensitivity tests to show  
98 that the GMPE approach we have taken produces similar results to the weighted-alternative GMPE  
99 approach, if the utilized information on available GMPE choices is treated consistently; it is the GMPE  
100 models and weights that are important, not the mechanics of how they are treated. These sensitivity  
101 tests are described in Atkinson (2012, Appendix B).

102

103 The underlying principles for the GMPEs that are proposed herein are as follows:

- 104 1. Median GMPEs should be selected from published (or peer-reviewed) equations.
- 105 2. The GMPEs will be given for a reference site condition ( $V_{s30}=760$  m/s, where  $V_{s30}$  is the time-  
106 averaged shear-wave velocity in the top 30 m). Models not available for B/C will be converted  
107 to an equivalent model for B/C.
- 108 3. The magnitude measure for the GMPEs is moment magnitude (**M**), and the GMPEs will be used  
109 with a revised Canadian earthquake catalog where various local magnitude values have all been  
110 converted to estimated **M**.
- 111 4. A variety of distance metrics may be used in the GMPEs. Point-source metrics may include  $R_{epi}$   
112 (epicentral distance) and  $R_{hypo}$  (hypocentral distance). Corresponding fault-distance metrics are  
113  $R_{jb}$  (Joyner-Boore distance, based on distance to surface projection of rupture plane), and  $R_{cd}$   
114 (closest distance to fault rupture surface), respectively. Fault-distance metrics may be converted  
115 to an equivalent point-source metric in the hazard software when needed (the need is software  
116 dependent); examples of such conversions are provided by Atkinson and Goda (2011) and  
117 Atkinson (2012).
- 118 5. Epistemic uncertainty in median GMPEs will be modeled by the use of alternative equations, as  
119 discussed above.
- 120 6. It is proposed for logistical convenience that a set of three alternative-weighted GMPEs will be  
121 used to describe the epistemic uncertainty; this includes a “lower”, “central” and “upper”  
122 GMPE, where each of the three is an alternative estimate of the median ground-motion  
123 amplitudes. Each alternative is given a specified weight for use in the hazard calculation (within  
124 logic tree enumeration or Monte Carlo simulation software).

- 125 7. The relative performance of the models, and a check on whether they fairly represent epistemic  
126 uncertainty, may be assessed by comparing the proposed GMPEs to each other, and to available  
127 ground-motion data adjusted to the B/C site condition, as appropriate.
- 128 8. We make an initial estimate of epistemic uncertainty for each GMPE type or region, then revisit  
129 the epistemic uncertainty across regions to ensure overall logical consistency, as well as  
130 agreement with key relevant datasets.
- 131 9. The random (or aleatory) variability about the median GMPE, often referred to as sigma, is  
132 treated as a separate issue from the specification of the median GMPEs and their epistemic  
133 uncertainty. Note that the discussion of aleatory uncertainty (“sigma”) follows the discussion of  
134 the epistemic uncertainty.

135

### 136 **Western crustal GMPEs**

137

138 A common assumption made for crustal earthquakes in B.C. is that their ground motions will be well  
139 represented by GMPEs for other active tectonic regions, such as California. Atkinson (2005) looked at  
140 this issue and concluded that, overall, observations of B.C. crustal earthquakes might be modeled (with  
141 some conservatism) using typical WNA crustal equations, if differences in predominant site conditions  
142 of the seismographs are accounted for – in particular the fact that much of B.C. has been glaciated while  
143 California has not. Our use of B/C as a reference site condition, however, means no conversion of  
144 GMPEs already defined in B/C will be required.

145

146 The suite of GMPEs currently favoured for crustal events in active tectonic regimes is the PEER-NGA  
147 equations (Power et al., 2008 and the references therein), due to its extensive and high-quality database  
148 (especially at the near-source distances important to hazard) from diverse active regions worldwide.  
149 (Note: the PEER-NGA equations are being updated in 2012-2013, but the new equations are not yet  
150 available.) A few challenges arise in using the PEER-NGA equations, some logistical and some  
151 scientific:

- 152 (1) many of them involve a level of detail in the parameter specifications that goes beyond what  
153 is available/reasonable for western Canada, leaving many parameters to be defined by default  
154 “guesses”;

- 155 (2) it is known that these GMPEs tend to over-estimate motions from events of  $M < 5.75$   
156 (Atkinson and Morrison, 2009; Chiou et al., 2010; Bommer et al. 2007; Cotton et al., 2008;  
157 Atkinson and Boore, 2011), but only two of the equations (BA08 and Chiou and Youngs)  
158 have published corrections for this effect (Chiou et al., 2010; Atkinson and Boore, 2011) –  
159 which can be important in low-to-moderate seismicity regions of B.C.;
- 160 (3) The GMPEs agree “too closely” with each other, and thus probably don’t actually convey the  
161 true epistemic uncertainty in median values (Abrahamson et al., 2008; Atkinson, 2011).  
162

163 To overcome these challenges, we define a three-equation suite that is based loosely on the PEER-NGA  
164 equations. We use the modified (for moderate-magnitude) BA08’ equations (Atkinson and Boore,  
165 2011) for “unspecified” fault mechanism as the central GMPE, as these are the simplest, and do not  
166 require specification of unknown variables. We use the other PEER-NGA equations to estimate the  
167 uncertainty bounds on these central equations. Figure 1 provides an example of the guidance for lower  
168 and upper alternatives to be defined about the central equation to reflect epistemic uncertainty; in this  
169 plot, the alternative equations of Boore and Atkinson, Abrahamson and Silva, Campbell and Bozorgnia,  
170 and Chiou and Youngs are plotted for PSA at several periods, for  $M=6.5$ , all for B/C conditions. To put  
171 the equations in an empirical perspective, the PEER-NGA data (also converted to B/C conditions, as per  
172 Boore and Atkinson, 2008) are plotted in magnitude bins 0.5 units in width, and in distance bins 0.4 log  
173 units in width. For the central magnitude value (e.g. 6.5), the mean and standard deviation of the log  
174 amplitudes within the bin is plotted. For magnitude bins 0.25 units less or greater than the central value,  
175 the means are plotted (without standard deviations, to avoid clutter); the magnitude bins have a 50%  
176 overlap. A series of such plots was made to examine the magnitude-distance range that is most  
177 important for hazard applications in western Canada. As noted in Abrahamson et al. (2008), the PEER-  
178 NGA equations are all fairly similar, and all are reasonably (though not perfectly) constrained by the  
179 data. A subjective judgment from Figure 1 (and similar figures) is that the epistemic uncertainty in  
180 median equations can be reasonably modeled by adding and subtracting 0.1 to 0.15 units  $\log(10)$  (25%  
181 to 40%) from the BA08’ equations, to give lower and upper alternative equations, respectively. This  
182 would encompass the PEER-NGA equations and most of the data constraints fairly well.

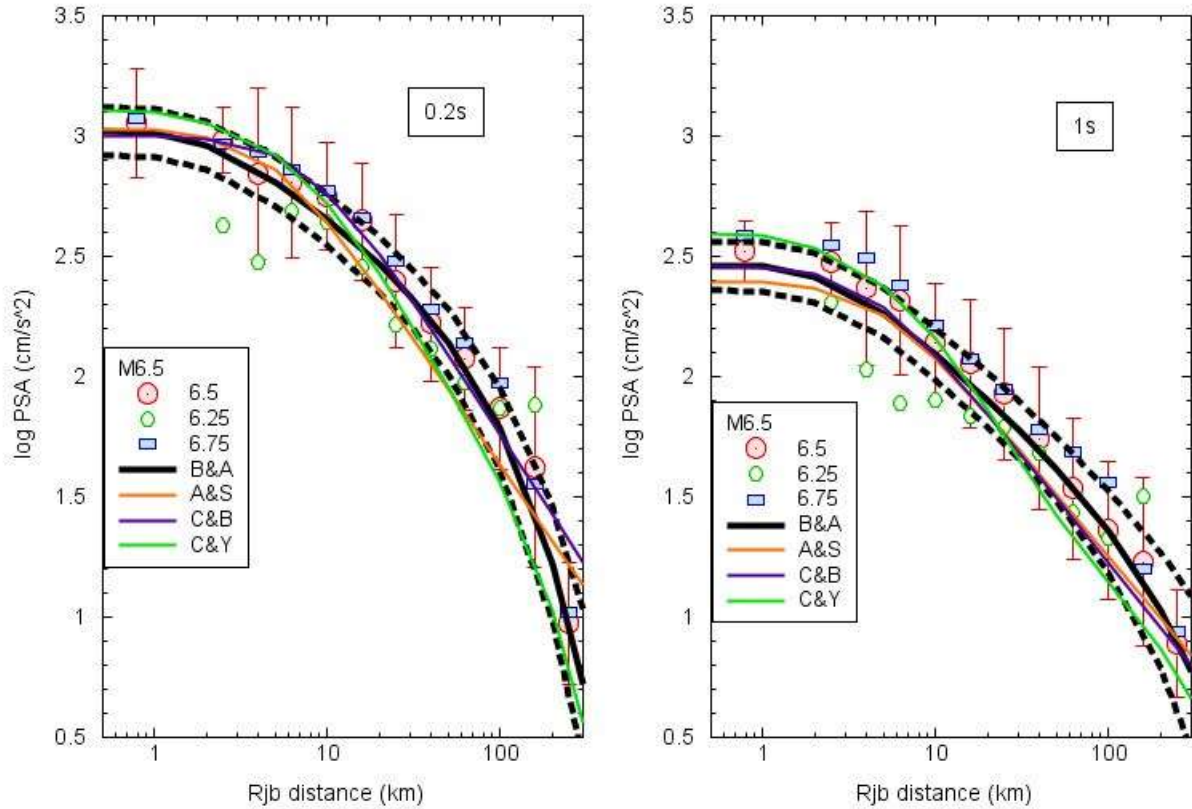
183  
184 It should be noted that use of this approach does not imply a preference for the BA08’ equations – all of  
185 the PEER-NGA equations have the same degree of validity. Rather, it is a convenience of application

186 that the PEER-NGA results may be encapsulated by taking BA08', the simplest of the models, as  
187 representative, and using factors about it to bracket the family of GMPEs.  
188 Looking carefully at GMPE plots for western crustal events (such as those shown in Atkinson (2012)) in  
189 both log and linear scale, for the  $M=6.5$  to  $7.5$  earthquakes that dominate seismic hazard in western  
190 Canada, it appears that uncertainty in the central GMPE, considering the alternative GMPEs and the data  
191 that constrain them, is of the order of  $0.15$  log units (factor of  $1.4$ ). This also takes some account of the  
192 fact that we are importing a global GMPE to western Canada. Furthermore, it appears that the  
193 uncertainty should grow with distance, based on the spread in the PEER-NGA equations; this is also  
194 appropriate given that the NGA equations combined data from different regions, having somewhat  
195 different attenuation rates. The following log factor ( $\delta$ ) is recommended to add/subtract from BA08'  
196 to express epistemic uncertainty through lower and upper alternative relations (this is the uncertainty  
197 plotted in Figure 1).

$$198 \quad \delta \text{ (crustal)} = \min (0.10 + 0.0007 R_{jb}, 0.3) \quad (\log_{10} \text{ units})$$

200  
201 Delta is "capped" at  $0.3$  log units (distance  $\sim 280$  km, at the edge of the plot) to prevent unreasonably  
202 large values at greater distances. Note that the resulting total uncertainty from the lower to upper GMPE  
203 is about a factor of  $2$  for the western crustal events. The factor of  $2$  should be considered a minimum  
204 uncertainty for other event types, because the western crustal GMPEs are the most-widely studied, and  
205 best-constrained by data. Recommended weights for the lower, central and upper alternatives for the  
206 western crustal events are  $0.25$ ,  $0.5$  and  $0.25$ , respectively.

207  
208



209

210 *Figure 1 – Proposed lower, central and upper GMPEs, for M6.5 crustal events in western Canada.*

211 *Solid black line is central equation (BA08’); dashed black lines are lower and upper equations, obtained*  
 212 *by adding and subtracting delta from the central equation. Solid lines show other PEER-NGA*  
 213 *equations. Symbols show means of the log amplitudes for various 0.5 unit magnitude bins; error bars*  
 214 *show standard deviation for the M6.5 magnitude bin.*

215

216 **Offshore crustal events**

217

218 Atkinson (2005) examined differences in ground motion source and attenuation properties for different  
 219 classes of events in B.C., and found that, relative to B.C. crustal onshore events: (i) those along the west  
 220 coast of Vancouver Island (just offshore) showed similar apparent source properties but steeper  
 221 attenuation; and (ii) the events far off-shore in oceanic crust have much lower apparent source  
 222 amplitudes, but a similar apparent attenuation. As the offshore events are not major hazard sources, we  
 223 can treat these characteristics in the following approximate manner for seismic hazard analysis.

224



225 For the events along the west coast of Vancouver Island – within 50 km of land – we use the crustal  
226 GMPEs. The use of crustal GMPEs will be conservative, as the actual attenuation for these events may  
227 be somewhat steeper. For offshore events (>50 km offshore), we follow the recommendation of  
228 Atkinson (2005) that the motions be approximated by using crustal GMPEs (and their associated  
229 weights), but with a reduction of 0.5 moment magnitude units. Thus if the actual moment magnitude of  
230 an offshore event is 7.0, we predict its ground motions using  $M=6.5$ . This is consistent with the  
231 observation (Ristau et al., 2003, 2005) that moment magnitudes are larger than the commonly-used  
232 Local magnitude (ML) of the catalogue. Specifically, Ristau et al. report that  $M = ML + 0.7$  for  
233 offshore events; we do not expect an exact equivalence between the  $M$ -ML discrepancy and the size of  
234 the adjustment needed to  $M$ , because log PSA does not scale with magnitude in a 1:1 manner.

235

236

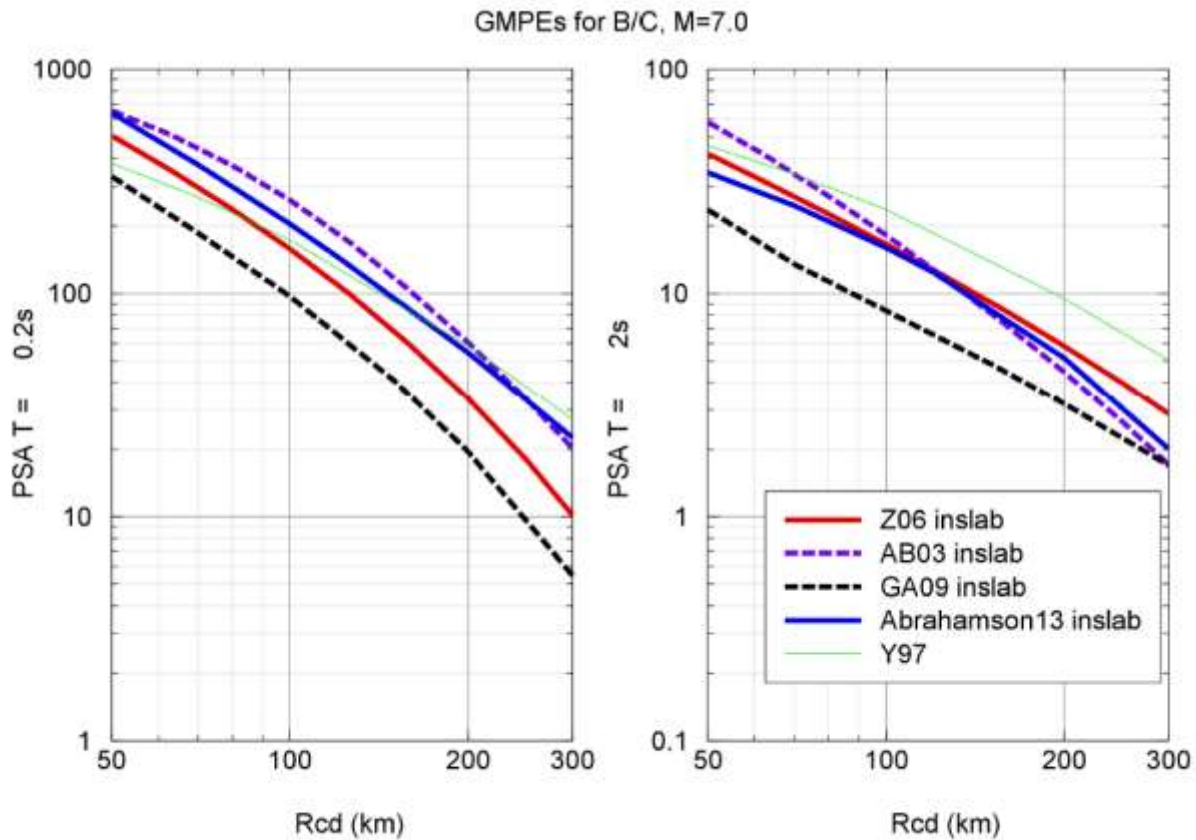
### 237 **Western subduction in-slab GMPEs**

238

239 Figure 2 compares several proposed GMPEs for subduction-zone in-slab events of  $M=7$ , including the  
240 Atkinson and Boore (2003) (AB03) GMPE for in-slab events (average of rock and C values are plotted to  
241 represent B/C conditions; Cascadia factor used), the Zhao et al. (2006) in-slab GMPEs for Japan (site  
242 class SC I, which is similar to B/C), the Goda and Atkinson (2009) GMPEs for deep events (>30 km) in  
243 Japan, and the median in-slab GMPE as developed by Abrahamson et al. (2013) (also referred to as the  
244 “BC Hydro GMPE model”). The classic Youngs et al. (1997) GMPEs (used in the 2005 and 2010  
245 hazard maps) are also shown for reference. Note that the attenuation rate given by the Y97 relations is  
246 relatively gentle, as it was pegged to match that for interface events (due to lack of in-slab data at the  
247 time the equations were developed). There appear to be large discrepancies between the alternative  
248 equations, but this is at least partly due to very different site conditions amongst the datasets employed,  
249 even for the same value of  $V_{s30}$ , as discussed in the next section.

250

251



252

253 *Figure 2: Comparison of alternative inslab GMPEs for M7 on B/C site: AB03 (Cascadia), Z06*  
 254 *(Japan), GA09 (Japan) and Abrahamson et al., 2013 (global). Y97(inslab) shown for reference. GMPEs*  
 255 *are given in  $cm/s^2$ .*

256

257 ***Modifications of GMPEs for inslab (and interface) to account for Cascadia site conditions***

258 Most of the recent global GMPEs for inslab and interface events are dominated by Japanese data,  
 259 because Japanese data are the most plentiful. It is known that shallow site conditions in Japan result in  
 260 amplification of short-period motions relative to long-period motions that is not captured by the use of  
 261  $V_{s30}$  or site class. Specifically, a NEHRP C site ( $V_{s30} \sim 550$  m/s) in Japan is typically a soft shallow soil  
 262 site (<20 m in depth) overlying much harder rock; this is markedly different from the more gradational  
 263 profiles typical of Californian recording sites. Detailed analyses of the 2011 M9 Tohoku ground  
 264 motions (Ghofrani et al., 2013) have shown that site amplifications in Japan for such sites are commonly  
 265 a factor of 5 or more at periods of 0.1-0.2 seconds. By contrast, site conditions in the much of the

266 Cascadia region are quite different (deeper soils), with more amplification at longer periods, but less at  
267 short periods. It is reasonable and prudent to adjust the GMPEs based on Japanese data to account for  
268 this factor.

269 A simple and transparent adjustment can be made based on the study by Atkinson and Casey (2003),  
270 which compared motions from two **M**6.8 inslab earthquakes, the Nisqually, Washington and Geiyo,  
271 Japan events, and showed that there is a period-dependent difference between the two that can be  
272 attributed to different typical site conditions, within the same site class. An important point to recall  
273 from the Atkinson and Casey study is that they also showed that the attenuation rates for inslab events  
274 are similar for Japan and Cascadia – thus the Japan-based GMPEs are appropriate for southwestern B.C.  
275 if suitable adjustments for site effects are made.

276 Atkinson and Casey showed that the discrepancies between the Geiyo and Nisqually motions disappear  
277 if we remove the expected regional site effects, computed from quarter-wavelength calculations for  
278 generic regional profiles for a given site class for the Nisqually event (factors in Table 2 of their paper).  
279 Thus to “convert” a Japan GMPE for Class C to an appropriate equivalent for Cascadia Class C, we  
280 multiply the predicted motions by a factor that is the ratio of (Cascadia NEHRP C/Japan NEHRP C).

281 An alternative approach is to use regional correction factors determined by regression analysis, such as  
282 those given by Atkinson and Boore (2003). Their Table 3 shows regional factors for Japan and  
283 Cascadia, which can be used to compute the ratio Cascadia/Japan, analogous to that computed by  
284 Atkinson and Casey. The difference is that the Atkinson and Boore factors were based on empirical data  
285 results (for Cascadia and Japan relative to the global average GMPEs), rather than computations for  
286 idealized soil profiles. Table 1 compares the factors suggested for the ratio Cascadia/Japan by these two  
287 alternative approaches; they are in good agreement with each other at most periods. It is proposed to  
288 use the average of the two results, shown as “Recommended” in Table 1 (both multiplicative and  $\log_{10}$   
289 factors shown). Linear interpolation in log-log space can be used for intermediate periods. The  
290 recommended soil correction factor damps motions for  $T < 0.4s$  and amplifies motions for  $T > 0.4s$ . Note  
291 that: (i) the amplification for PGV is assumed to be the same as that for  $T = 0.4s$ ; and (ii) the  
292 amplification factor is assumed to return to unity at very long periods.

293

294

295

296

297 *Table 1 – Factors to convert Japanese GMPEs to Cascadia GMPEs, for the same value of  $V_{s30}$ .*

Period (s)	Atkinson&Casey (2003)	Atkinson&Boore (2003)	Recommended Cascadia Multiplicative Factor (log units)
10			1.00 (0.000)
5			1.10 (0.040)
3		1.23	1.20 (0.079)
2	1.47	1.55	1.51 (0.179)
1	1.08	1.00	1.04 (0.017)
0.4	1.16	0.83	1.00 (0.000)
0.3			0.81 (-0.091)
0.2	0.71	0.50	0.60 (-0.222)
0.1	0.53	0.35	0.44 (-0.357)
0.04		0.35	0.44 (-0.357)
PGA		0.45	0.50 (-0.301)
PGV			1.00 (0.000)

298

299 The site correction factors of Table 1 should be applied to both inslab and interface GMPEs that are  
300 based predominantly on Japanese data, in order to obtain corresponding GMPEs for Cascadia. We  
301 determined that when this is done, the inslab GMPEs of AB03, Z06 and GA09 become very similar at  
302 short periods (0.1s and PGA) – the adjustment for regional site conditions brings them into close  
303 agreement. In the following discussion, we have removed regional site effects in our comparisons of  
304 GMPEs and data.

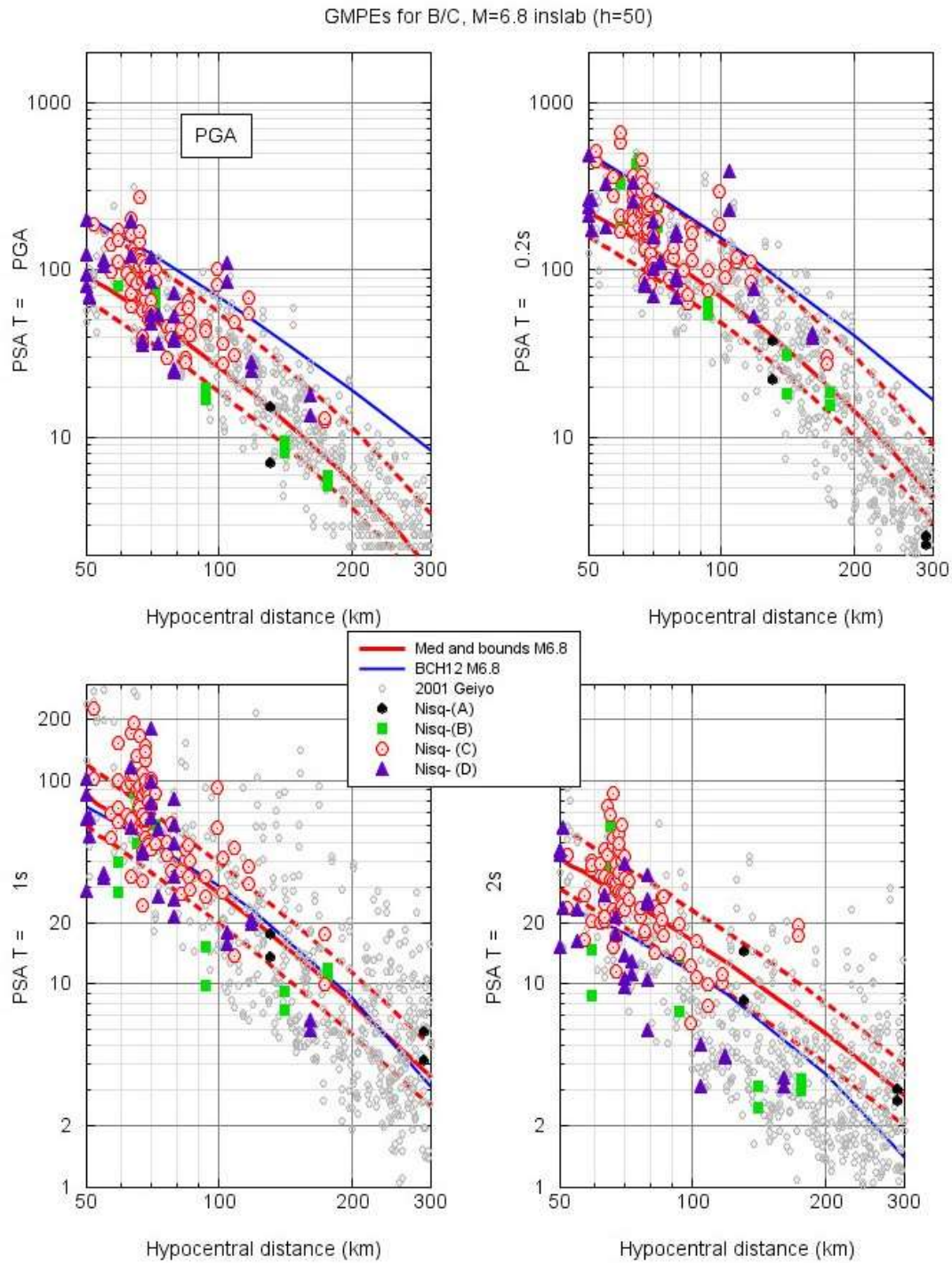
305 It is unclear whether regional site corrections should be applied to the Abrahamson et al. (2013) GMPEs,  
306 as they included a broad mix of regions in their database. They looked at the issue of regionalization by  
307 evaluating average event residuals by region, and considered these regional terms in the evaluation of  
308 epistemic uncertainty. Overall, they did not report recommendations for region-based adjustments to

309 their global model. However, they noted that the Cascadia region had significantly low average  
310 residuals at short periods relative to their global model; this finding is consistent with Table 1. We have  
311 plotted the global result of Abrahamson et al. (2013) when showing their GMPE for comparison,  
312 because they did not specifically recommend a modification for Cascadia. However, it may be noted  
313 that if their average regional event terms for Cascadia were applied, their GMPE would be reduced by  
314 about 0.17 log units at short periods (0.2 s to PGA).

315 We propose to use the Z06 GMPEs as the central GMPE, after adjustment for Cascadia site conditions,  
316 with the other equations being used to guide the choice of an epistemic uncertainty band about it. We  
317 assign an initial distance-independent uncertainty of 0.15 log units to represent lower and upper  
318 equations. This uncertainty is about the same as for Cascadia crustal earthquakes on average, and less  
319 than that proposed (below) for interface events. We modify the upper representative equation based on  
320 consideration of relevant data, as described in the following.

321 We evaluate how well the proposed suite represents relevant ground-motion data in Figure 3. The  
322 included data for the Cascadia region data are from the 2001 **M**6.8 Nisqually earthquake (in slab event,  
323 depth=50km). These data, taken from Atkinson and Boore (2003), are adjusted to B/C site conditions,  
324 using the conversions of Boore and Atkinson (2008) with an assumed  $V_{s30}$  of 450 m/s for C and 250  
325 m/s for D. We supplement the Cascadia data by considering also data from the **M**6.8 Geiyo event in  
326 Japan (also an in slab event at depth=50km), with the amplitudes adjusted to B/C conditions using the  
327 factors in Table 1. Figure 3 shows the lower, central and upper GMPE equations proposed for in slab  
328 events of **M**6.8 on B/C (at a focal depth of 50 km) in comparison to relevant data, and also to the  
329 proposed central GMPE of Abrahamson et al. (2013). The upper equation of our proposed suite was  
330 increased by a factor of 1.5 at periods  $\leq 0.2$ s (including PGA), because we noted that the data at short  
331 periods tended to be larger than those predicted by our initial proposed suite. (Note: the proposed  
332 multiplicative factor on the upper curve tapers from 1.5 to 1.0 as the period increases from 0.2s to 1s.)  
333 The revised upper GMPE curve (after increase by the factor of 1.5) is in reasonable agreement with  
334 Abrahamson et al. (2013). At intermediate periods (1 s) our central GMPE is very similar to that of  
335 Abrahamson et al. (2013). At long periods our central GMPE is larger than that of Abrahamson et al.  
336 (2013), but in reasonable agreement with the relevant data. In view of the data comparison in Figure 3,  
337 the proposed weights for the lower, central and upper GMPE branches are 0.25, 0.5, 0.25 for periods  $\geq 1$ s,

338 respectively. For periods  $\leq 0.2s$  (including PGA), the corresponding weights are 0.2, 0.4, 0.4, with a  
 339 transition of weights taking place between 1 and 0.2s (e.g. for 0.5s use 0.25, 0.4, 0.35).



340

341 *Figure 3 –Proposed lower, central and upper inslab GMPEs (in cm/s<sup>2</sup>) based on Zhao et al., 2006 (red*  
 342 *lines) and central GMPE of Abrahamson et al., 2013 (blue line) for M=6.8 inslab events, in comparison*

343 *to data from M6.8 events in Cascadia (Nisqually) and Japan (Geiyo). GMPEs for B/C site condition; all*  
344 *data adjusted to B/C as discussed in text.*

345

### 346 **Western subduction interface GMPEs**

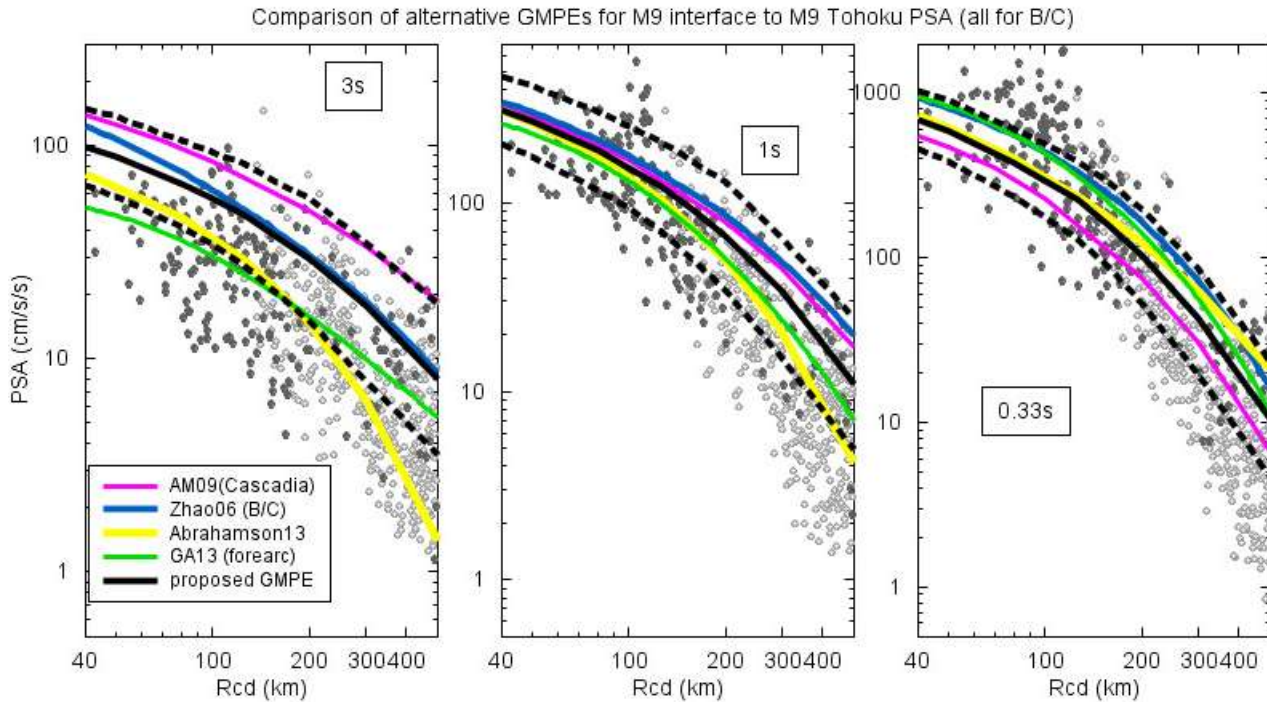
347

348 For interface events, both empirical and simulation-based GMPEs may be used to model the expected  
349 Cascadia mega-thrust motions. Zhao et al. (2006), Abrahamson et al. (2013) and Ghofrani and Atkinson  
350 (2013) provide empirical GMPEs for interface events, while Gregor et al. (2002) and Atkinson and  
351 Macias (2009) both use a simulation-based model to derive GMPEs from stochastic finite-fault  
352 simulations. The methodology used by Gregor et al. and Atkinson & Macias is similar, but the Atkinson  
353 and Macias (2009) GMPE is calibrated based on larger, more recent interface events (the M8.1 Tokachi-  
354 Oki event), and is developed for the reference condition of B/C boundary (the Gregor et al. equations are  
355 given for “rock” or “soil”, but the specified rock Vs30 is only 363m/s, which is significantly softer than  
356 B/C). The use of simulations is important for Cascadia subduction events due to the lack of recorded  
357 data for the expected type of event (M>8.5 with Cascadia attenuation).

358

359 An important factor to consider in selecting GMPEs for great interface earthquakes in Cascadia is new  
360 information from the 2011 M9 Tohoku earthquake, which was very well recorded. This is the type of  
361 event, and approximate magnitude, expected for future great earthquakes on the Cascadia subduction  
362 zone. The motions from Tohoku were very large, especially at short periods. This was partly due to  
363 pronounced site response effects (Ghofrani et al., 2013), similar to those already discussed. Figure 4  
364 compares the M9 Tohoku data, corrected to B/C site conditions (from Ghofrani and Atkinson, 2013) to  
365 several candidate GMPEs (for B/C). The empirical GMPE of Ghofrani and Atkinson (2013) included  
366 the Tohoku data directly in the regression, whereas the Abrahamson et al. (2013) GMPE used a global  
367 database, then subsequently tuned the GMPE following the occurrence of the Tohoku event. It should  
368 be kept in mind that the Tohoku data from distances >150 km are all from back-arc sites, which is why  
369 the attenuation for Tohoku at larger distances is quite steep (see Ghofrani and Atkinson, 2011). In  
370 Cascadia, a gentler attenuation is expected to apply for cities in southwestern B.C., which lie in the fore-  
371 arc region. We have not proposed a back-arc correction for sites east of the Cascade volcanic sequence  
372 in B.C., because no studies of this effect in B.C. have been performed, and it is not clear that the effect

373 in B.C. is as pronounced as that in Japan. Neglecting this potential effect is a source of conservatism in  
 374 the ground motions estimated for a Cascadia event in the interior regions of B.C.



375  
 376 *Figure 4 – Interface GMPEs in  $\text{cm/s}^2$  for 3, 1 and 0.33 s for  $M=9$ , in comparison to data for the  $M9$*   
 377 *Tohoku PSA data (Ghofrani and Atkinson, 2013), all for  $V_{s30}=760\text{m/s}$ ; dark symbols are forearc data,*  
 378 *light circles are backarc data. Zhao et al. (2006)GMPE is corrected to B/C from C assuming C*  
 379 *corresponds to  $V_{s30}\sim 450\text{ m/s}$ . Abrahamson et al. (2013) is plotted for fore-arc sites. AM09 (Atkinson*  
 380 *and Macias, 2009) is based on simulations for Cascadia; the central GMPE, based on a weighted*  
 381 *combination of the three candidate GMPEs as described in the text, is shown (heavy black line) along*  
 382 *with lower and upper representative equations that display our estimate of its epistemic uncertainty*  
 383 *(dashed black lines).*

384  
 385 Figure 4 shows that the simulation-based GMPE of AM09 predicts significantly-higher motions at long  
 386 periods, and lesser motions at short periods relative to the other equations and to the Tohoku data. We  
 387 place significant weight on the AM09 equation as it is a simulation-based model that is specific to  
 388 Cascadia site and attenuation conditions, but calibrated using Japanese ground-motion records. It agrees  
 389 reasonably well with the Tohoku motions at intermediate periods, after considering the differences  
 390 between fore-arc and back-arc attenuation. However, we note that the AM09 GMPE is conservative



391 relative to the Tohoku data and to the alternative GMPEs at long periods (3s plot in Fig. 4). We are not  
392 certain whether the AM09 GMPE is indeed an over-estimate, or whether the Tohoku data may not have  
393 been representative of a “typical” M9 interface event. The Tohoku event was a complex multiple event,  
394 that was comprised of multiple ruptures, whose sum made up its total moment. We also note that the  
395 AM09 GMPE tends to be low relative to the Abrahamson et al. (2013) and Ghofrani and Atkinson  
396 (2013) GMPEs at short periods ( $\leq 0.2$ s).

397  
398 In view of these considerations, the preferred central GMPE for interface events is developed by taking  
399 a weighted average of the candidate GMPE motions for forearc regions, giving 50% weight to the  
400 simulation-based GMPE motions of Atkinson and Macias (2009), with the remaining weight to  
401 empirical GMPEs. We give 20% weight to Abrahamson et al. (2013), 20% weight to Ghofrani and  
402 Atkinson (2013), and a lesser weight of 10% to Zhao et al. (2006) (noting that the Zhao et al. model  
403 does not consider the more recent Tohoku data). Because the Ghofrani and Atkinson (2013) and Zhao et  
404 al. (2006) models were based exclusively on Japanese data, they were corrected to Cascadia site  
405 conditions by applying the Japan-to-Cascadia factors as given in Table 1 before combining with the  
406 Atkinson and Macias (2009) Cascadia model and the Abrahamson et al. (2013) global model. Note that  
407 this is the central-model GMPE that is plotted in Figure 4 (i.e. as constructed from the weighted average  
408 of the log amplitudes).

409  
410  
411  
412 It is proposed that the uncertainty in GMPEs for interface events should grow with distance, as was the  
413 case for the crustal GMPEs. However, the overall uncertainty should exceed that for crustal events. We  
414 have no ground-motion information specific to Cascadia on the motions from this type of event, and  
415 therefore the uncertainty must be larger than that for crustal events. We propose uncertainty bounds  
416 with which to construct lower and upper GMPE curves (relative to the central GMPE of AM09) as:

417  
418 
$$\text{delta (interface)} = \min( (0.15+0.0007 Rcd), 0.35) \quad (\log_{10} \text{ units})$$

419  
420 This will provide a factor of 2.8 in amplitude scaling from the lower to the upper GMPE, at 100 km  
421 (growing to a factor of 5.2 at 300 km). The uncertainty will be 0.05 log units larger than that for crustal

422 events in the west. Recommended weights for the lower, central and upper GMPEs are 0.25, 0.5 and  
423 0.25, respectively.

424

#### 425 **Eastern GMPEs (crustal)**

426

427 The definition of appropriate GMPEs for eastern North America (ENA) is challenging due to the lack of  
428 relevant data in the magnitude-distance range of most interest. We propose to use GMPEs of several  
429 different types (differing classes of approaches) that have been developed for ENA within the last  
430 decade, as an initial estimate of the epistemic uncertainty. The proposed GMPEs are summarized below  
431 (in reverse chronological order of publication); we include only relations that are useable over the entire  
432 magnitude/distance range of needed for seismic hazard map computations ( $M_{4.8}$  to 8 at distances to 600  
433 km).

434

435 *PZT11: Pezeshk, Zhandieh and Tavakoli, 2011*

436 The PZT11 GMPE is based on the hybrid empirical approach developed by Campbell (2003), but uses  
437 an updated model for both the ENA parameters and the reference equations from western North  
438 America (WNA). The idea is that a stochastic point-source model is used to derive adjustment factors  
439 for WNA GMPEs, based on differences in model inputs between ENA and WNA. The parameter values  
440 are simple and well-motivated.

441

442 The PZT11 GMPE is specified for hard-rock site conditions, so must be converted to B/C site  
443 conditions. PZT11 used the Atkinson and Boore (2006) (AB06) values of amplification and kappa for  
444 ENA hard rock (~2000m/s), and the corresponding values from Boore and Joyner (1997) for WNA rock  
445 (~600m/s), in their model to derive correction factors from WNA to ENA. This follows the approach to  
446 amplification factors used by AB06, and therefore we can use conversion factors from A to B/C based  
447 on AB06 to predict the corresponding B/C motions for the PZT11 model (from their hard-rock GMPE  
448 values).

449

450 Under this approach, constant values (in log<sub>10</sub> units) can be added to the hard-rock predictions (for  
451 log<sub>10</sub>(PSA)) of PZT11 to get equivalent predictions for B/C, as given in Table 2. The conversions were  
452 derived by plotting the differences (in log<sub>10</sub> units) between the predictions of AB06 on B/C and those on

453 A, and noting they are insensitive to magnitude. The factors listed are for  $M=6$ , but would be only about  
 454 0.02 units lower for  $M=5$ , or 0.02 units higher for  $M=7$ ; this is trivial given other uncertainties. The  
 455 factors are also insensitive to distance, except for very short periods ( $<0.03s$ ) and PGA; a distance-  
 456 dependent factor is given for PGA (which can also be used for 0.025s PSA). The distance variable in  
 457 PZT11 is closest distance to the fault ( $R_{cd}$ ).

458

459 *Table 2 – Conversion factors in log10 units from A to B/C site conditions for PZT11 GMPE*

PSA:period(s)	A to B/C
5	0.06
2	0.09
1	0.11
0.5	0.14
0.33	0.14
0.2	0.12
0.1	0.03
0.05	-0.1
PGV	0.09
PGA*	$-0.3+0.15\log(\text{Repi})$

460

461 \* PGA value may also be used for PSA at  $T \leq 0.025s$ .

462

463 *AB06'*: Atkinson and Boore, 2006 (as revised in Atkinson and Boore, 2011)

464 The AB06' GMPE model is based on a stochastic finite-fault approach, which is a simulation approach  
 465 that uses a seismological model, with key parameters calibrated based on ENA ground-motion data. It is  
 466 one of a very small number of recent published ENA GMPEs that includes both a comprehensive model  
 467 and a comprehensive comparison of the model against ENA data. Coefficients are provided for both  
 468 B/C and hard-rock conditions, so we can use the B/C version directly. The equations were updated  
 469 (Atkinson and Boore, 2011) to agree better with moderate-magnitude ground-motion amplitude data,  
 470 and with WNA-scaling of motions with magnitude. The updated version is referred to as AB06'.

471

472 The distance variable in AB06' is  $R_{cd}$ . Care should be taken in converting to  $R_{cd}$  from hypocentral  
 473 distance as the AB06 model does not build in distance-saturation effects, but instead relies on keeping

474 the fault a reasonable distance away (i.e. the assumption of a buried fault) to avoid this problem.  
475 Atkinson and Boore (2011) recommend using a minimum depth to the top of the rupture ( $Z_{\text{tor}}$ ) that  
476 depends on magnitude, in order to place minimum constraints on the value of  $R_{\text{cd}}$  that is associated with  
477 near-epicentre distances and hence ensure distance-saturation of near-fault amplitudes. These minimum  
478 values for  $R_{\text{cd}}$  should be applied following the conversion, if necessary. (e.g.  $R_{\text{cd}}$  is the value given by  
479 the conversion equations from  $R_{\text{hypo}}$ , but constrained such that  $R_{\text{cd}}(\text{min}) = Z_{\text{tor}} = 21 - 2.5 \mathbf{M}$ ; in other  
480 words, if the calculated value of  $R_{\text{cd}}$  is less than  $(21 - 2.5\mathbf{M})$ , we use  $(21 - 2.5\mathbf{M})$  in its place.) Note this  
481 minimum value decreases from  $R_{\text{cd}}(\text{min}) = 8.5 \text{ km}$  at  $\mathbf{M}5$  to  $R_{\text{cd}}(\text{min}) = 2.3 \text{ km}$  at  $\mathbf{M}7.5$ .

482

483 *A08': Atkinson, 2008 (as revised in Atkinson and Boore, 2011)*

484 The A08' GMPE is based on a referenced empirical approach, which is similar in concept to the hybrid  
485 empirical approach, but uses ENA data directly to derive adjustment factors to WNA GMPEs. It is a  
486 useful inclusion from the point of view of epistemic uncertainty as it suggests a smoother attenuation  
487 function than do model-based approaches (like AB06' and PZT11). Coefficients are provided for B/C  
488 conditions. The distance metric is closest distance to the surface projection of the rupture ( $R_{\text{jb}}$ ). This  
489 model was recently updated by Atkinson and Boore (2011) to use modified BA08' GMPEs for WNA  
490 (see sections below) as the reference; these modifications account for recent moderate-magnitude  
491 observations in both ENA and WNA. The modified version is referred to as A08'.

492

493 *SGD02S: Silva, Gregor and Daragh, 2002, Single-corner (variable stress)*

494 This GMPE has never been formally published (except on the authors' website) but has been very  
495 widely used; it is recommended for consideration for this reason, as an 'industry-standard' stochastic  
496 point-source model (in which stress drop decreases with magnitude to mimic WNA saturation effects).  
497 It is given for hard-rock conditions, so must be converted to B/C; the conversion factors of Table 2 can  
498 be used for this purpose, as the amplification model employed by the authors is very similar to that of  
499 AB06. The distance variable is  $R_{\text{jb}}$ .

500

501 *SGD02D: Silva, Gregor and Daragh, 2002, Double-corner (with saturation)*

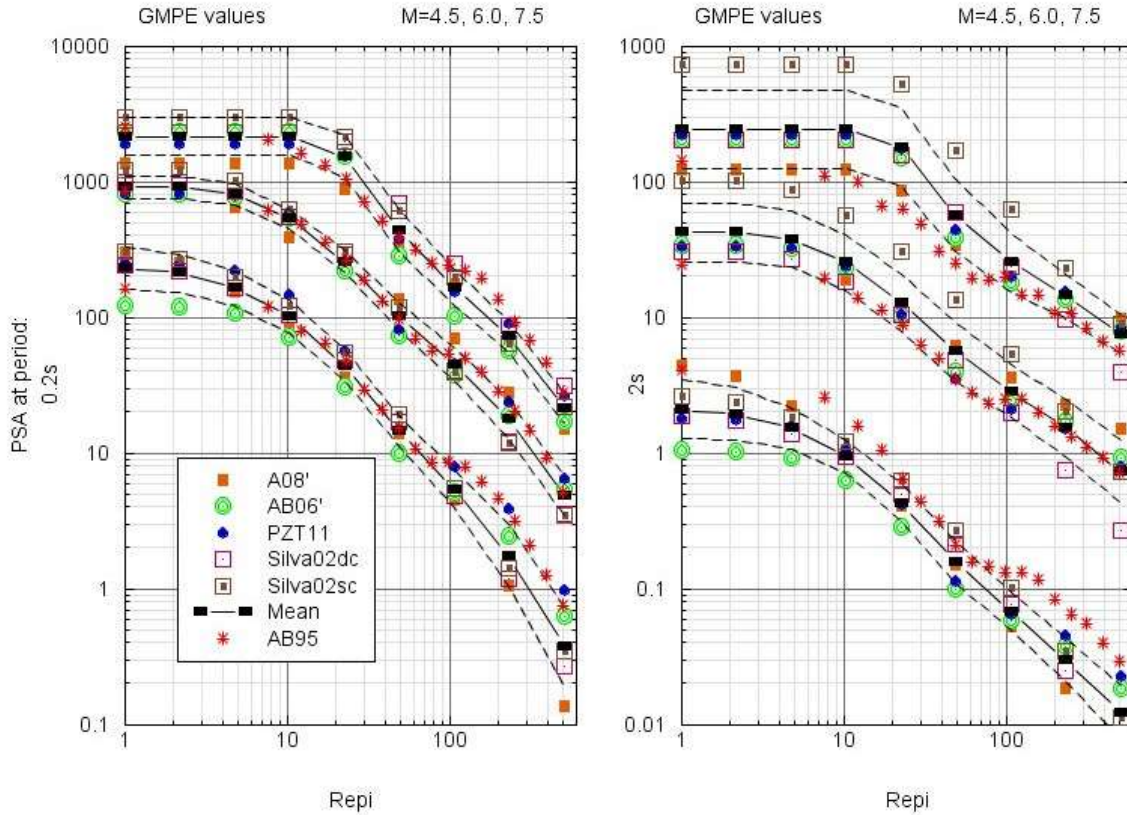
502 This is another variant of the SGD02 model, in which a double-corner stochastic point-source model is  
503 used in the simulations, to consider epistemic uncertainty in source. As for the SGD02S model, it needs  
504 to be converted to B/C, and the distance metric is  $R_{\text{jb}}$ .

505

506 We implement the five ENA GMPEs by defining a suite of three relationships for the ground motions,  
507 for each magnitude-distance-period, that express the geometric mean and its standard deviation (where  
508 the geometric mean is the arithmetic average of the five log values of the median ground motions from  
509 the alternative relations). The mean and mean  $\pm$  one standard deviation define the central, lower and  
510 upper curves. A conversion from the distance metric of each GMPE to epicentral distance is made using  
511 a simple approximation, assuming ENA fault dimensions, as a point-source metric is required for the  
512 hazard calculations (see Appendix A of Atkinson 2012 for details). We smooth the standard deviation  
513 using a triangular 3-point weighted smoothing, to avoid “pinching” of the lower and upper bounding  
514 relations at certain distances where the five estimates fortuitously happen to lie close together. The sets  
515 of GMPEs are implemented in a table format in the hazard software, so that no “fitting” to the values is  
516 required (the table in log PSA vs. log distance is interpolated to find the value corresponding to any **M**,  
517 distance and period); the tables are available on the author’s website ([www.seismotoolbox.ca](http://www.seismotoolbox.ca) ).

518

519 Figure 5 shows the central GMPE from the five candidate relations, along with the corresponding lower  
520 and upper GMPEs. The Atkinson and Boore (1995) equations, used in the NBCC (2005, 2010) maps,  
521 are shown for reference (converted to B/C). The epistemic uncertainty obtained using this procedure  
522 varies with magnitude, distance and period, with a typical average value being 0.17 log<sub>10</sub> units (factor of  
523 1.5).



524

525 *Figure 5: PSA values in  $cm/s^2$  at 0.2s and 2s (for  $M=4.5, 6.0, 7.5$ ) for five ENA GMPEs versus*  
 526 *epicentral distance, along with geometric mean values (black squares), proposed central GMPE (solid*  
 527 *black line), and relations giving mean  $\pm$  standard deviation (dashed black lines). Red asterisks show*  
 528 *values from the AB95 equations, which were used in the 2005, 2010 NBCC maps.*

529

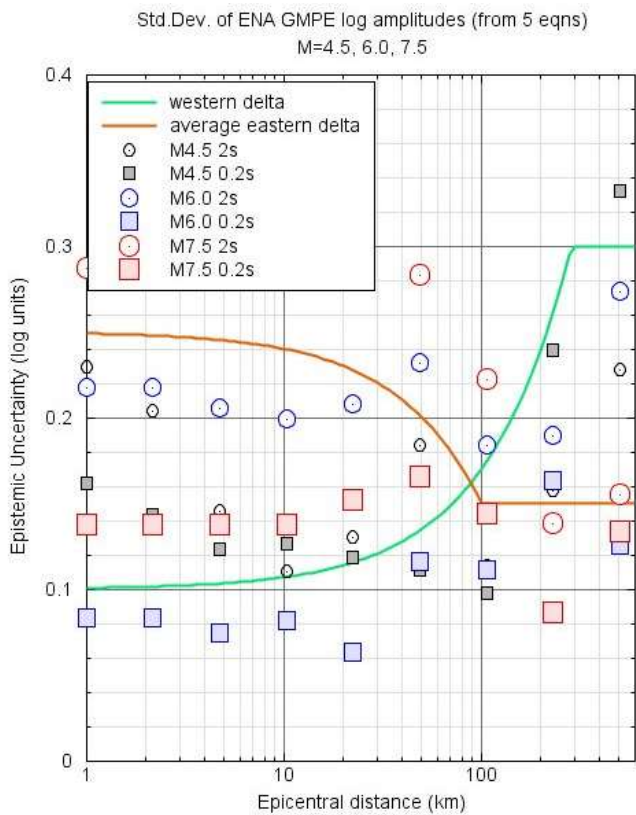
530 In Figure 6, the standard deviation of the median GMPE predictions for the east is plotted versus  
 531 distance for  $M$  4.5, 6.0 and 7.5, for 2s and 0.2s. Generally, the implied uncertainty from the standard  
 532 deviation of the GMPEs is larger than the value adopted for western crustal GMPEs, but not always.  
 533 Overall, the impression is that the eastern GMPEs should carry larger epistemic uncertainty, in  
 534 comparison to the western crustal equations. Furthermore, in the east the ground motions are most  
 535 constrained by data and studies at regional distances, and should be considered most uncertain at close  
 536 distances, due to the paucity of relevant near-source observational data. This pattern of uncertainty  
 537 behavior with distance is different than that for the west. This suggests that additional uncertainty  
 538 should be provided, above that given by the standard deviation of log amplitudes about the central  
 539 GMPE. We add an additional epistemic uncertainty to modify the GMPE+std and GMPE-std equations

540 for the east, having greatest effect at close distances. The uncertainty (log units to add to GMPE+std,  
 541 and subtract from GMPE-std) is:

542  $\text{delta (ENA GMPE+std, GMPE-std)} = \max( (0.1 - 0.001 R_{\text{epi}}), 0.0)$

543 This will increase the epistemic uncertainty above that given by the standard deviation of the geometric  
 544 mean of the eastern GMPEs by 0.1 (factor of 1.26) at close distances, such that its typical value would  
 545 be ~0.2 for short periods and 0.35 for long periods. It would leave the uncertainty unchanged for  
 546  $R_{\text{epi}} > 100$  km. The average value (over all magnitudes and periods) is shown in Figure 6, in comparison  
 547 to the western crustal uncertainty. The recommended weights for the lower, central and upper  
 548 alternatives are 0.25, 0.5 and 0.25, respectively.

549



550

551 *Figure 6 – Standard deviation (in log units) of mean of 5 eastern GMPEs by magnitude and distance for*  
 552 *2s and 0.2 Hz (symbols). Recommended eastern epistemic uncertainty adds 0.1 to these plotted values at*  
 553 *close distances (reducing to no additional uncertainty for  $R_{\text{epi}} > 100$ km). Green line shows recommended*  
 554 *epistemic uncertainty for western crustal events. Orange line shows general behaviour of the eastern*  
 555 *epistemic uncertainty.*

556

557 **Comparison of GMPEs across regions**

558

559 It is useful to compare the GMPEs to each other across regions. Figure 7 plots the response spectra, for  
560 B/C conditions, for **M7** events at epicentral distances of approximately 10 and 100 km. This plot is  
561 indicative of the size of events that contribute to hazard across a broad range of periods for typical  
562 Canadian seismic hazard mapping applications. To facilitate comparisons, we have calculated the  
563 weighted mean of the GMPE suite for each event type, which is what is shown in Figure 7. This shows  
564 that the event types are all scaling in a similar way with period, though there are some significant  
565 differences in amplitude levels. At short periods, eastern events show larger amplitudes than western  
566 crustal events, as we would expect based on the observations for events in the east, which are typically  
567 modeled by higher stress drops. The amplitudes expected for subduction interface events are generally  
568 similar to those for crustal events, at least at the **M7** level. Inslab events have lower amplitudes at short  
569 epicentral distances, because they are actually further away, due to their focal depths (~50 km);  
570 however, at epicentral distances for which the focal depth effect is less important, the relatively-large  
571 amplitudes for inslab events at short periods become more apparent.

572

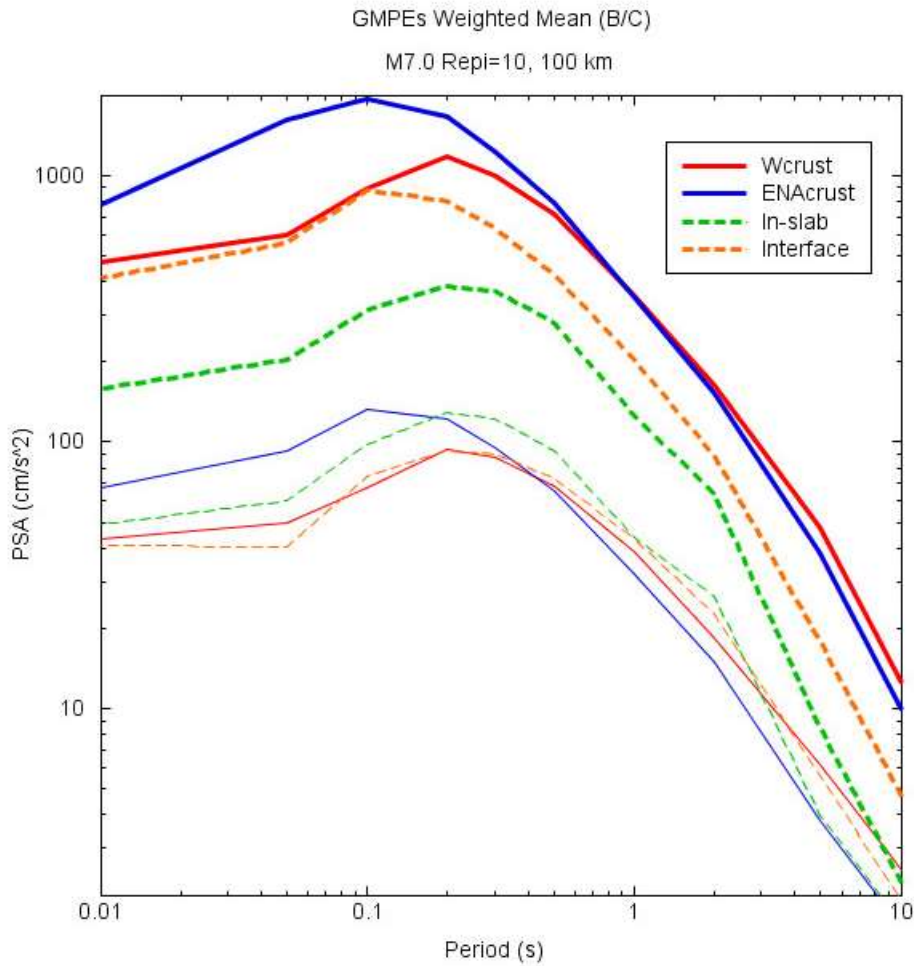
573 We examined plots such as those shown on Figure 7 for a range of magnitudes, but for brevity have  
574 shown only one example here. Inspection of such plots gives us confidence that the GMPEs are  
575 internally-consistent in the way they behave when compared across regions.

576

577

578





579  
 580 *Figure 7 – Response spectrum in cm/s<sup>2</sup> for M7 events at epicentral distances of 10 (heavy lines), 100 km*  
 581 *(light lines), for four different event types, for B/C conditions.*

582

583 **Aleatory Variability in GMPEs (Sigma)**

584

585 The value of sigma (aleatory variability, or random scatter of observations about a GMPE) to be  
 586 associated with the GMPEs is an important parameter. Traditionally, sigma was assigned based on  
 587 observed variability about the regression equation (statistics of misfit to the equations). More recently,  
 588 it has been realized that this may not be the appropriate way to define sigma, as what we are trying to  
 589 capture is natural variability in future events, as opposed to total variability in regression - which  
 590 includes factors such as model misfits, variable soil conditions, data errors and so on. These factors all  
 591 contribute to reported values for regression statistics, but are not representative of actual physical

592 variability. There is also potential for some double-counting of aleatory uncertainty when epistemic  
593 uncertainty in the median equations is included in the hazard analysis. These issues have been discussed  
594 in papers by Anderson and Brune (1999), Anderson et al. (2000), Abrahamson and Bommer (2005),  
595 Atkinson (2006, 2011) and Strasser et al., (2009). Atkinson (2011) shows that actual variability in  
596 amplitudes within well-recorded events is about 0.22 log(10) units at long periods ( $>1s$ ), decreasing to  
597 about 0.20 units at short periods ( $\leq 0.25s$ ). This includes just the within-event variability, and also  
598 implicitly includes variability in site conditions for a given value of  $V_{s30}$  (due to differing soil depths,  
599 etc.). Based on the PEER-NGA equations, typical inter-event variability values decrease from about  
600 0.16 to 0.12 units over the same period range; note that the inter-event variability includes any regional  
601 variability in source characteristics, in addition to actual event-to-event variability within a specific  
602 region. Considering these values, representative values for a multi-site sigma would be about 0.27  
603 log(10) units at long periods ( $\geq 1s$ ), decreasing to 0.23 units at short periods ( $\leq .25s$ ); note that single-  
604 station sigma values (Atkinson, 2006, 2013) would be lower. The representative values are obtained  
605 from the inter-event and intra-event components using the standard square-root-sum-of-squares rule. It  
606 is proposed that these sigma values be applied to all event types and regions, as there is no definitive  
607 evidence that sigma varies with region (see Atkinson, 2013), and sigma is best defined for western  
608 crustal events. The proposed sigma values are slightly smaller than the corresponding range of 0.25  
609 (short period) to 0.30 (long period) quoted by Boore and Atkinson (2008) based on their regression  
610 results; this is in accord with our view that the assigned aleatory uncertainty should be less than  
611 indicated by regression statistics to avoid double-counting of aleatory and epistemic uncertainty.

612

### 613 **Conclusion**

614

615 This study has suggested suites of lower, central and upper GMPEs for each type of event for use in  
616 seismic hazard mapping in Canada. The use of the 3 sets of GMPEs is a simple and efficient way to  
617 represent epistemic uncertainty in GMPEs. The implications of this approach, including comparisons  
618 with more traditional approaches such as using a variety of alternative published GMPEs without  
619 modification, are explored in separate investigations. To date, these investigations have shown that the  
620 three-equation approach is equivalent to the use of multiple GMPEs, provided the same range of  
621 epistemic uncertainty is sampled.

622

623 **Acknowledgements**

624

625 We have benefited from discussions with the ground-motion modeling group of the Canadian Standing  
626 Committee on Earthquake Design, including in particular Garry Rogers, Tuna Onur, Liam Finn and  
627 Adrian Wightman. Karen Assatourians provided computational assistance. The review comments of  
628 Paul Somerville on our GMPE choices are gratefully acknowledged, along with constructive reviews  
629 from Trevor Allen and two anonymous reviewers. The first author's research is supported by the  
630 National Sciences and Engineering Research Council.

631

632 **References**

633

- 634 Abrahamson, N. and J. Bommer (2005). Probability and uncertainty in seismic hazard analysis.  
635 Earthquake Spectra, **21**, 603-608.
- 636 Abrahamson, N., G. Atkinson, D. Boore, Y. Bozorgnia, K. Campbell, B. Chiou, I. Idriss, W. Silva and  
637 R. Youngs (2008). Comparison of the NGA Ground-Motion Relations. Earthquake Spectra, **24**, 45-  
638 66.
- 639 Abrahamson, N., N. Gregor and K. Addo (2013). B.C. Hydro Ground Motion Prediction Equations for  
640 Subduction Earthquakes. Earthquake Spectra, submitted.
- 641 Adams, J. (2011). Seismic Hazard Maps for the National Building Code of Canada. Canadian Society of  
642 Civil Engineers General Conference - Ottawa, Ontario June 14-17, 2011, paper JHS-1-1.
- 643 Adams, J. and S. Halchuk (2003). Fourth generation seismic hazard maps of Canada: Values for over  
644 650 Canadian localities intended for the 2005 National Building Code of Canada, Geological Survey  
645 of Canada Open File 4459, 155 pp.
- 646 Anderson, J. and J. Brune (1999). Methodology for using precarious rocks in Nevada to test seismic  
647 hazard models. Bull. Seism. Soc. Am., **89**, 456-467.
- 648 Anderson, J., J. Brune, R. Anooshehpour and S. Ni (2000). New ground motion data and concepts in  
649 seismic hazard analysis. Current Science, **79**, 1278-1290.
- 650 Atkinson, G. (1995). Ground motion relations for use in eastern hazard analysis. In Proceedings, 7th  
651 Canadian Conference on Earthquake Engineering, Montreal, June 1995, p. 1001-1008.
- 652 Atkinson, G. (2005). Ground motions for earthquakes in southwestern British Columbia and  
653 northwestern Washington: crustal, in-slab, and offshore events, *Bull. Seism. Soc. Am.* **95**, 1027-1044.

654 Atkinson, G. (2006). Single-station sigma. *Bull. Seism. Soc. Am.*, **96**, 446-455.

655 Atkinson, G. M. (2008). Ground-motion prediction equations for eastern North America from a  
656 referenced empirical approach: implications for epistemic uncertainty, *Bull. Seism. Soc. Am.* **98**,  
657 1304-1318.

658 Atkinson, G. (2011). An empirical perspective on uncertainty in earthquake ground motions. *Can.J.Civil*  
659 *Eng.*, **38**,1-14. DOI:10.1139/110-120.

660 Atkinson, G. (2012) White paper on development of ground-motion prediction equations for Canadian  
661 National Seismic Hazard Maps. [www.seismotoolbox.ca](http://www.seismotoolbox.ca) (Misc. Resources). Nov. 2012.

662 Atkinson, G. (2013). Empirical evaluation of aleatory and epistemic uncertainty in eastern ground  
663 motions. *Seism. Res. L.*, **84**, 130-138.

664 Atkinson, G., and D. Boore (1995). New ground motion relations for eastern North America. *Bull.*  
665 *Seism. Soc. Am.*, **85**, 17-30.

666 Atkinson, G. M., and D. M. Boore (2003). Empirical ground-motion relations for subduction-zone  
667 earthquakes and their application to Cascadia and other regions, *Bull. Seism. Soc. Am.* **93**, 1703-1729.

668 Atkinson, G. M., and D. M. Boore (2006). Earthquake ground-motion prediction equations for eastern  
669 North America, *Bull. Seism. Soc. Am.* **96**, 2181-2205.

670 Atkinson, G. and D. Boore (2011). Modifications to existing ground-motion prediction equations in light  
671 of new data. *Bull. Seism. Soc. Am.*, **101**, 1121-1135.

672 Atkinson, G. M., and R. Casey (2003). A comparison of ground motions from the 2001 **M** 6.8 inland  
673 earthquakes in Cascadia and Japan, *Bull. Seism. Soc. Am.* **93**, 1823-1831.

674 Atkinson, G. and K. Goda (2011). Effects of seismicity models and new ground motion prediction  
675 equations on seismic hazard assessment for four Canadian cities. *Bull. Seism. Soc. Am.*, **101**, in  
676 press.

677 Atkinson, G. M., and M. Macias (2009). Predicted ground motions for great interface earthquakes in the  
678 Cascadia subduction zone, *Bull. Seism. Soc. Am.* **99**, 1552-1578.

679 Atkinson, G. and M. Morrison (2009). Regional variability in ground motion amplitudes along the west  
680 coast of North America. *Bull. Seism. Soc. Am.*, **99**, 2393-2409.

681 Bommer, J., N. Abrahamson, F. Strasser, A. Pecker, P. Bard, H. Bungum, F. Cotton, D. Fah, F. Sabetta,  
682 F. Scherbaum and J. Studer (2004). The challenge of defining upper bounds on earthquake ground  
683 motions. *Seism. Res. L.*, **75**, 82-95.

684 Bommer, J., P. Stafford, J. Alarcon and S. Akkar (2007). The influence of magnitude range on empirical

685 ground-motion prediction. *Bull. Seism. Soc. Am.*, **97**, 2152-2170.

686 Bommer, J. and F. Scherbaum (2008). The use and misuse of logic trees in probabilistic seismic hazard  
687 analysis. *Earthquake Spectra*, **24**, 997-1009.

688 Boore, D. and G. Atkinson (2008). Ground-motion prediction equations for the average horizontal  
689 component of PGA, PGV, and 5%-damped SA at spectral periods between 0.01s and 10.0 s.  
690 *Earthquake Spectra*, **24**, 99-138.

691 Boore, D. and W. Joyner (1997). Site amplifications for generic rock sites. *Bull. Seism. Soc. Am.*, **87**,  
692 327-341.

693 Boore, D. W. Joyner and T. Fumal (1997). Equations for estimating horizontal response spectra and  
694 peak acceleration from western North American earthquakes: A summary of recent work.  
695 *Seism. Res. L.*, **68**, 128-153.

696 Campbell, K. W. (2003). Prediction of strong ground motion using the hybrid empirical method and its  
697 use in the development of ground-motion (attenuation) relations in eastern North America, *Bull.*  
698 *Seism. Soc. Am.* **93**, 1012-1033.

699 Chiou, B., R. Youngs, N. Abrahamson and K. Addo (2010). Ground motion model for small-to-  
700 moderate shallow crustal earthquakes in California and its implications for regionalization of ground  
701 motion prediction models. *Earthquake Spectra*, **26**, 907-926.

702 Cotton, F., G. Pousse, F. Bonilla, and F. Scherbaum (2008). On the Discrepancy of Recent European  
703 Ground-Motion Observations and Predictions from Empirical Models: Analysis of KiK-net  
704 Accelerometric Data and Point-Sources Stochastic Simulations, *Bulletin of the Seismological Society*  
705 *of America*, **98**(5), 2244-2261.

706 Ghofrani, H. and G. Atkinson (2011). Fore-arc versus back-arc attenuation of earthquake ground  
707 motion. *Bull. Seism. Soc. Am.*, **101**, 3032-3045.

708 Ghofrani, H. and G. Atkinson (2013). Ground-motion prediction equations for interface earthquakes of  
709 M7 to 9 in Japan based on empirical data. *Bull. Earthq. Eng.*, submitted.

710 Ghofrani, H., G. Atkinson and K. Goda (2013). Implications of the 2011 M9.0 Tohoku Japan earthquake  
711 for the treatment of site effects in large earthquakes. *Bull. Earthq. Eng.*, in press.

712 Goda, K., and G. M. Atkinson (2009). Probabilistic characterization of spatially correlated response  
713 spectra for earthquakes in Japan, *Bull. Seism. Soc. Am.* **99**, 3003-3020.

714 Goda, K., H. Hong and G. Atkinson (2010). Impact of using updated information on seismic hazard in  
715 Western Canada. *Can. J. Civil Eng.*, **37**, 562-575.

716 Gregor, N. , W. Silva, I. Wong, and R. Youngs (2002). Ground-motion attenuation relationships for  
717 Cascadia subduction zone megathrust earthquakes based on a stochastic finite-fault model, *Bull.*  
718 *Seism. Soc. Am.* **92**, 1923-1932.

719 Pezeshk, S., A. Zandieh and B. Tavakoli (2011). Ground-motion prediction equations for eastern North  
720 America from a hybrid empirical method. *Bull. Seism. Soc. Am.*, in review.

721 Power, M., Chiou, B., Abrahamson, N, Y. Bozorgnia, T. Shantz and Roblee, C. (2008). An overview of  
722 the NGA project. *Earthquake Spectra*, **24**, 3-21.

723 Ristau, J., G. Rogers, and J. Cassidy (2003). Moment magnitude-local magnitude calibration for  
724 earthquakes off Canada's west coast, *Bull. Seism. Soc. Am.* **93**, 2296- 2300.

725 Ristau, J., G. Rogers, and J. Cassidy (2005). Moment magnitude-local magnitude calibration for  
726 earthquakes in western Canada, *Bull. Seism. Soc. Am.* **95**, 1994-2000.

727 Scherbaum, F., J. Schmedes, and F. Cotton (2004). On the conversion of source-to-site distance  
728 measures for extended earthquake source models, *Bull. Seism. Soc. Am.* **94**, 1053-1069.

729 Silva, W. J., N. J. Gregor, and R. Darragh (2002). *Development of regional hard rock attenuation*  
730 *relations for central and eastern North America*, Technical Report, Pacific Engineering and Analysis,  
731 El Cerrito, CA. [www.pacificengineering.org](http://www.pacificengineering.org).

732 Somerville, P., N. Collins, N. Abrahamson, R. Graves and C. Saikia (2002). Ground motion attenuation  
733 relations for the central and eastern United States. Report to U.S. Geological Survey (NEHRP).

734 Strasser, F., N. Abrahamson and J. Bommer (2009). Sigma: Issues, insights and challenges. *Seism. Res.*  
735 *L.*, **80**, 40-56.

736 Youngs, R. R., S. J. Chiou, W. J. Silva, and J. R. Humphrey (1997). Strong ground motion attenuation  
737 relationships for subduction zone earthquakes, *Seism. Res. Lett.* **68**, 58-73.

738 Zhao, J. , J. Zhang, A. Asano, Y. Ohno, T. Oouchi, T. Takahashi, H. Ogawa, K. Irikura, H. Thio, P. G.  
739 Somerville, Y. Fukushima, and Y. Fukushima (2006). Attenuation relations of strong ground motion  
740 in Japan using site classification based on predominant period, *Bull. Seism. Soc. Am.* **96**, 898-913.

741